International Journal of Mass Spectrometry 294 (2010) 93–102

Contents lists available at ScienceDirect

International Journal of Mass Spectrometry

journal homepage: www.elsevier.com/locate/ijms

Complex fragmentation pathways of rhodanine and rhodanine-3-acetic acid upon resonant capture of low-energy electrons

Stanislav A. Pshenichnyuk[a,*], Alberto Modelli[b,c]

[a] Institute of Physics of Molecules and Crystals, Ufa Research Center, Russian Academy of Sciences, October Avenue, 151, 450075 Ufa, Russia
[b] Dipartimento di Chimica "G. Ciamician", Universitá di Bologna, via Selmi 2, 40126 Bologna, Italy
[c] Centro Interdipartimentale di Ricerca in Scienze Ambientali (CIRSA), Universitá di Bologna, via S. Alberto 163, 48123 Ravenna, Italy

ARTICLE INFO

Article history:
Received 7 April 2010
Received in revised form 19 May 2010
Accepted 21 May 2010
Available online 1 June 2010

Keywords:
Dissociative electron attachment
DEA spectra
Metastable negative ions
Rhodanine

ABSTRACT

A detailed gas-phase study of dissociative electron attachment (DEA) to rhodanine (**Rd**) and its 3-acetic acid derivative (**Rdaa**) in the 0–14 eV energy range has been carried out with a magnetic mass spectrometer under conditions of medium energy resolution (0.4 eV) of the incident electron beam, and high sensitivity. The DEA spectra reveal the occurrence of numerous and complex dissociative decay channels of the molecular anions formed by resonances, involving multiple bond cleavage and structural rearrangements. Along with a variety of anion fragments normally formed in the collision cell at incident electron energies <1 eV, dissociation of a series of metastable anion species (occurring in the time scale of microseconds) is also detected. The observation of these slow processes is consistent with the complexity of many dissociative channels, and allows to propose schemes for the fragmentation pathways. The DEA spectra of both **Rd** and **Rdaa** also display small yields of molecular anions at zero energy. Their lifetimes with respect to electron detachment are experimentally evaluated to be about 30 μs and 200 μs, respectively. These (vibrationally excited) ground anion states formed by capture of thermal electrons mainly into the ring π* (C═S) LUMO survive long enough to redistribute their excess energy before undergoing different dissociation channels.

1. Introduction

The electron-acceptor rhodanine (**Rd**) derivative rhodanine-3-acetic acid (**Rdaa**, see Chart 1) was found to be a promising candidate for dye-sensitized solar cell components [1]. However, a recent electron transmission spectroscopy (ETS) [2] and dissociative electron attachment spectroscopy (DEAS) [3] study [4] showed that attachment of slow electrons to these compounds is followed by dissociation, thus casting serious doubts on their long-term stability under conditions of excess negative charge.

The aim of the present study is to get more insight into the complex dissociation channels which follow low-energy resonant electron capture in the above mentioned gas-phase molecules. This investigation was performed by means of the electron attachment spectroscopy (EAS) technique using a magnetic mass filter [5] in the 0–14 eV incident electron energy range. Setting the instrumental sensitivity as high as possible, some decay channels of the molecular anion that escaped detection in the former study [4] could be revealed. Most importantly, the present experimental equipment can reveal fragmentation pathways which involve formation of metastable anions, i.e., dissociation processes which take place in a time scale of the order of magnitude of microseconds. The structures and yields of some negative fragments could be determined taking advantage of isotopic analysis.

2. Experiment

Our EAS apparatus coupled with a negative ion mass spectrometer has been previously described [5,6]. Briefly, a magnetically collimated electron beam is passed through a collision cell filled with a gas of the substance under investigation. A current of mass-selected negative ions formed inside the collision cell by resonant electron attachment is recorded as a function of the incident electron energy. The accessible electron energy range is 0–14 eV, and the electron beam saturation current is 1 μA. The electron energy scale is calibrated with the SF_6^- signal at zero energy under attachment of thermal electrons to SF_6. The full width at half-maximum of the electron energy distribution is estimated to be 0.3–0.4 eV, and the accuracy of the measured peak energies ±0.1 eV.

Evaluation of the electron detachment time is based on detection of the neutral species formed by electron detachment from negative ions during their flight through the field-free region between the mass analyzer and the secondary electron multiplier. This method, previously proposed [7] for time-of-flight experi-

* Corresponding author.
E-mail address: sapsh@anrb.ru (S.A. Pshenichnyuk).

1387-3806/$ – see front matter © 2010 Elsevier B.V. All rights reserved.
doi:10.1016/j.ijms.2010.05.025

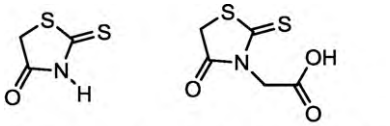

Chart 1.

ments, can be modified for magnetic mass spectrometers [5]. In the present experimental equipment the lifetimes required for detection through the mass filter are about 26 μs and 29 μs for the **Rd** and **Rdaa** molecular anions, respectively.

A sufficient sample pressure in the collision cell, under single-collision conditions, was obtained heating **Rd** ($C_3H_3NOS_2$) and **Rdaa** ($C_5H_5NO_3S_2$) at 80 and 90 °C, respectively. The temperature of the walls of the collision cell was kept at 90 °C in both cases. The samples are commercially available (Aldrich).

Geometry optimizations and evaluation of total energies were performed with the Gaussian 03 set of programs [8], using the B3LYP hybrid functional [9] with the standard 6–31+G(d) basis set.

3. Results

3.1. Negative ions formed by resonant electron capture

3.1.1. Rhodanine

Fig. 1 shows the most intense anion currents generated by electron attachment to gas-phase **Rd**. The results are in good agreement with an earlier DEA investigation [4] carried out using an apparatus with a higher energy resolution of the incident electron beam, but a smaller sensitivity. The measured peak energies and relative intensities are listed in Table 1. The most intense current (m/e = 91, peaking at 0.6 eV) is due to loss of a ketene (H_2CCO) molecule. The peak at 0.9 eV in the yield of the **Rd** molecular anion (m/e = 133) is entirely (intensity and shape) accounted for by isotopic contributions (about 5.4%) from the more intense m/e = 132 dehydrogenated anion, peaking at the same energy.

Many other negative fragments generated by dissociation of the parent anion of **Rd** were detected. Their intensities are smaller than that of the m/e = 91 anion fragment by several orders of magnitude (see Table 1). Currents of these negative ions, as a function of the

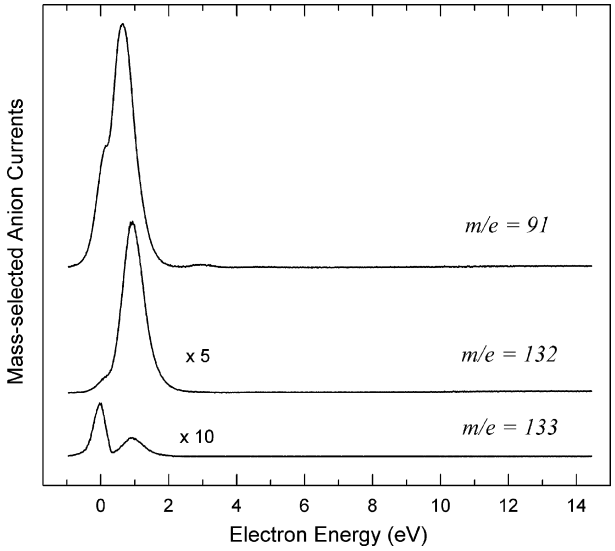

Fig. 1. Most intense mass-selected anion currents, as a function of the incident electron energy, formed by DEA to gas-phase **Rd**.

Table 1
Peak energies (eV) and relative intensities (evaluated from the peak heights) of the anion currents measured in the DEA spectrum of rhodanine (**Rd**) at 90 °C.

m/e	Anion structure	Peak energy (eV)	Relative intensity
26	$[CN]^-$	0.0	<0.1
		1.7	<0.1
		3.2	0.13
		4.5	0.15
		9.2	<0.1
32	$[S]^-$	0.2	<0.1
		3.2	0.16
		4.5	0.31
		6.3 sh.	
33	$[SH]^-$	0.0	0.10
		1.8 sh.	
		3.2	<0.1
		4.5	0.10
37.0	m_1^*: 91 → 58	0.0 sh.	
		0.6	<0.1
		3.0	<0.1
40	$[CCO]^-$	3.0	<0.1
		4.4	<0.1
41	$[CHCO]^-$	3.4	<0.1
		4.4	0.10
42	$[OCN]^-$	3.2	0.23
		4.5	0.51
45	$[SCH]^-$	0.6	<0.1
		4–6 broad	<0.1
		8.1	<0.1
46	$[CH_2S]^-$	0.0	<0.1
		3.1	0.29
		4.4	0.51
57	$[Rd–CS_2]^-$	1.3	<0.1
		3.1	0.31
		4.4 sh.	
58	$[SCN]^-$	0.0 sh.	
		0.6	0.42
		3.1	2.55
		4.4	3.01
60	$[OCS]^-$	3.1	0.10
		4.3	0.10
62.3	m_2^*: 133 → 91	0.0	<0.1
		0.7	<0.1
64	$[S_2]^-$	0.0	<0.1
		3.1	<0.1
		4.5	0.10
72	$[SCCO]^-$	0.0	<0.1
		1.2	<0.1
		3.0	0.11
		4.4	0.10
73	$[Rd–OCS]^-$	3.2	0.10
		4.6	0.14
		7.9	<0.1
74	$[SCH_2CO]^-$	0.0	<0.1
		1.0	<0.1
		3.0	<0.1
		4.5	<0.1
75	[Rd–SCN]-	0.0	0.10
		0.6 sh.	
76	$[CS_2]^-$	0.9	<0.1
		3.2 sh.	
		4.5	<0.1
		6.3 sh.	
91	$[Rd–H_2CCO]^-$	0.0 sh.	
		0.6	100
		3.0	1.00
100	$[Rd–SH]^-$	0.7	<0.1
		3.0	0.18
105	$[Rd–CO]^-$	0.0 sh.	
		1.0	0.27
132	$[Rd–H]^-$	0.0 sh.	
		0.9	13.9
133	$[Rd]^-$, 30 μs	0.0	2.14

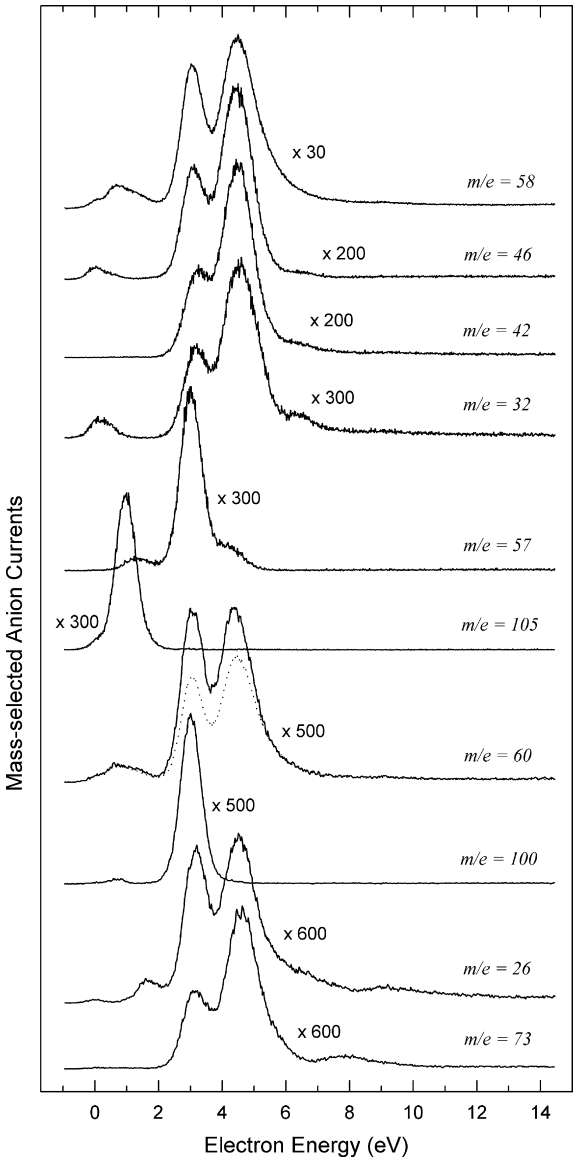

Fig. 2. Mass-selected anion currents, as a function of the incident electron energy, formed by DEA to gas-phase **Rd**. The intensities of these currents are smaller than that of the *m/e* = 91 current by one or two orders of magnitude. Isotopic contributions from the *m/e* = 58 to the *m/e* = 60 yield are shown by a dotted line.

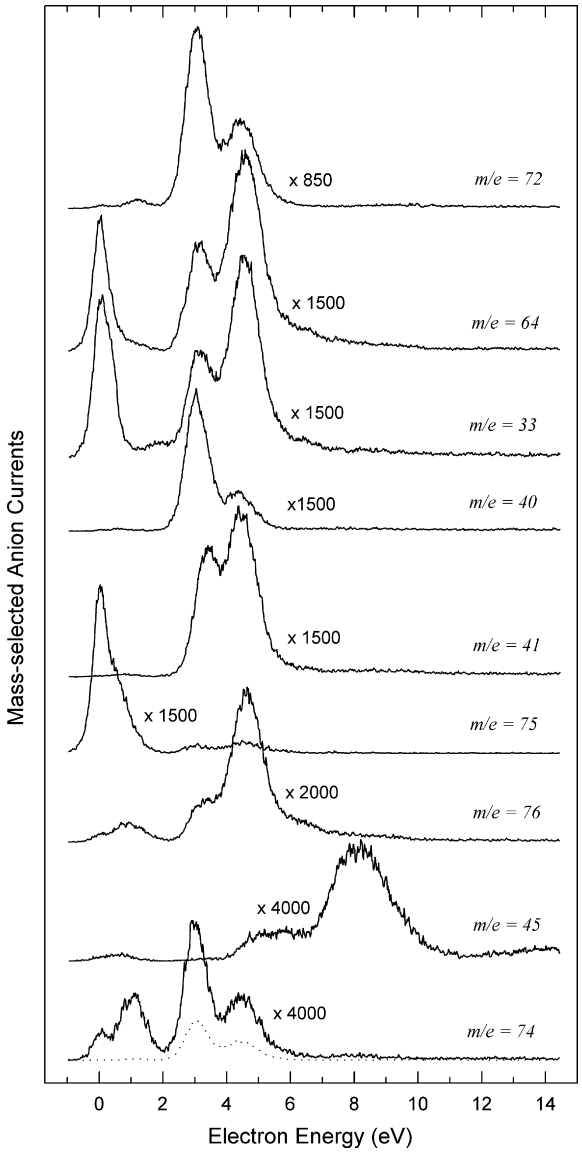

Fig. 3. Mass-selected anion currents, as a function of the incident electron energy, formed by DEA to gas-phase **Rd**. The intensities of these currents are smaller than that of the *m/e* = 91 current by two or three orders of magnitude. Isotopic contributions from the *m/e* = 72 to the *m/e* = 74 yield are shown by a dotted line.

incident electron energy, are shown in Figs. 2 and 3, in order of decreasing yield (the intensity scale is the same as that of Fig. 1). Peak energies and relative intensities are listed in Table 1 in order of increasing mass number.

Possible assignments of the observed anion currents to the corresponding negative fragments are given in Table 1. Due to the presence of a variety of heteroatoms, the formation of many small negatively charged species via dissociative electron attachment to **Rd** is not surprising, as observed for instance in the case of the heterocyclic 6-aza-2-thiothymine molecule [10]. The observed mono- di- and tri-atomic fragment anions are $[CN]^-$ (*m/e* = 26), $[SCN]^-$ (*m/e* = 58), $[OCN]^-$ (*m/e* = 42), $[S]^-$ (*m/e* = 32), $[SH]^-$ (*m/e* = 33), $[SCH]^-$ (*m/e* = 45), $[S_2]^-$ (*m/e* = 64), $[CS_2]^-$ (*m/e* = 76) and $[CCO]^-$ (*m/e* = 40).

The *m/e* = 60 anion yield at 3.0 and 4.5 eV is mostly due to isotopic contributions (4.4%, plotted in Fig. 2 with a dotted line) from the more intense *m/e* = 58 current. The remaining yield can be due to $[OCS]^-$ or $[CH_2SN]^-$. Formation of either fragment requires the occurrence of strong rearrangements. In fact, both include atoms which are not adjacent in the parent negative ion. The *m/e* = 46 current is likely to be ascribed to $[CH_2S]^-$ or (less probably, accounting for isotopic abundances and the *m/e* = 47 relative intensity) to the $[SN]^-$ anion. The zero energy shoulder in the *m/e* = 76 current is completely due to isotopic contributions from the *m/e* = 75 negative fragment.

Several of the above mentioned small negative fragments are also formed as neutral species, leaving the negative charge on the corresponding $[Rd–fragment]^-$ counterpart, namely, $[Rd–SCN]^-$ (*m/e* = 75), $[Rd–SH]^-$ (*m/e* = 100), $[Rd–CS_2]^-$ (*m/e* = 57), $[Rd–OCS]^-$ (*m/e* = 73). The small maxima at 3.0 and 4.5 eV in the *m/e* = 75 current are completely accounted for by isotopic contributions from the *m/e* = 73 anions. The most plausible structure of the *m/e* = 72 anion is $[SCCO]^-$. Its isotopic contribution (4.6%) to the *m/e* = 74 species is not enough to cover the measured yield of the latter, as shown in Fig. 3 by a dotted line, thus suggesting the formation of the $[SCH_2CO]^-$ fragment. The anion fragment with *m/e* = 105 corresponds to loss of a carbonyl group from the molecular anion, $[Rd–CO]^-$, although its $[CO]^-$ counterpart has not been detected.

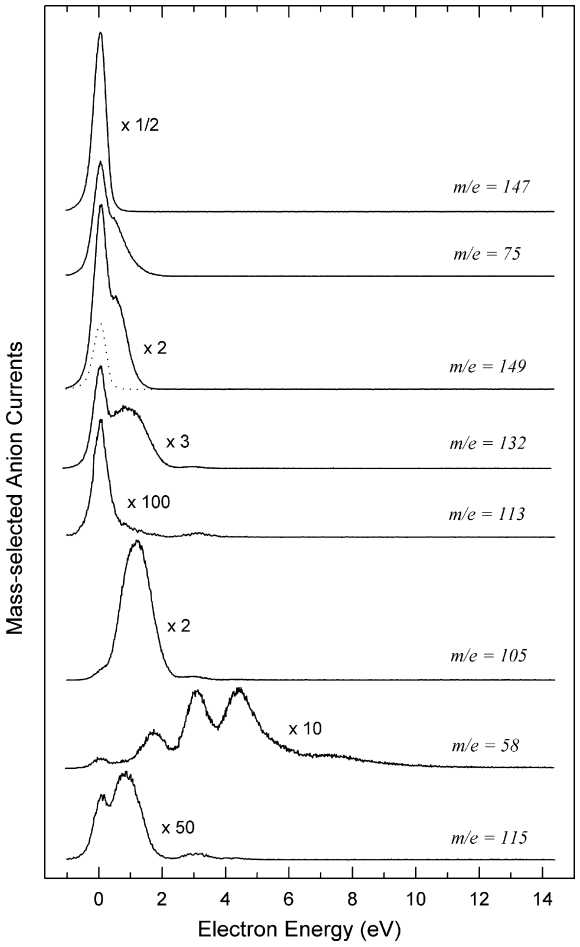

Fig. 4. Most intense mass-selected anion currents, as a function of the incident electron energy, formed by DEA to gas-phase **Rdaa**. Isotopic contributions from the *m/e* = 147 to the *m/e* = 149 yield are shown by a dotted line.

Most of the weak negative currents observed in the DEA spectra of **Rd** (see Figs. 2 and 3) show two pronounced peaks at incident electron energies of about 3.0 and 4.5 eV. The former has a counterpart in the total anion current [4], where a broad and relatively weak signal was observed at the same energy, and in the ET spectrum, where a distinct resonance is displayed at 3.1 eV [4]. According to B3LYP calculations, this resonance is associated with electron capture into a ring antibonding σ^*_{CS} MO [4]. Fragment anion currents are also observed in the 5–6 eV energy range (*m/e* = 32, 45 and 76) and around 8 eV (*m/e* = 45 and *m/e* = 73), as shown in Figs. 2 and 3. These low-intensity negative fragments observed above 4 eV likely originate from core-excited resonances [3], i.e., two electron processes where electron capture is accompanied by a valence electron excitation. To verify this point, we performed TD-B3LYP/6–31+G* calculations [11] to evaluate the first excitation energies of the vertical anion state of **Rd**. The n–π^* and π–π^* excited states result to lie 3.87 and 4.01 eV, respectively, above the ground anion state. Accounting for a calculated vertical electron affinity of 0.51 eV, the energy thresholds for formation of the corresponding core-excited anions are predicted to be about 3.4 and 3.5 eV.

3.1.2. Rhodanine-3-acetic acid

Fig. 4 shows some mass-selected fragment anion currents generated by DEA to gas-phase **Rdaa**, in close agreement with those reported previously [4]. The measured peak maxima and relative intensities are listed in Table 2 , in order of increasing mass num-

Table 2
Peak energies (eV) and relative intensities (evaluated from the peak heights) of the anion currents measured in the DEA spectrum of rhodanine-3-acetic acid (**Rdaa**) at 90 °C.

m/e	Anion structure	Peak energy (eV)	Relative intensity
17	$[OH]^-$	5.7	<0.1
		~8	<0.1
26	$[CN]^-$	0.0	<0.1
		1.7	<0.1
		4.5	<0.1
		~8	<0.1
32	$[S]^-$	0.0 sh.	
		0.5	<0.1
		3.1	0.12
		4.4	0.10
33	$[SH]^-$	3.1	0.53
		4.3	0.61
38.3	m_3^*: 147 → 75	0.0	0.10
40	$[CCO]^-$	3.1	<0.1
		4.5	<0.1
		~6–9 broad	<0.1
41	$[CHCO]^-$	3.1 sh.	
		4.6	0.10
		~8	<0.1
42	$[OCN]^-$	1.4	<0.1
		3.2	<0.1
		4.6	<0.1
		~6–9 broad	<0.1
46	$[CH_2S]^-$	0.0	<0.1
		1.6	0.10
		3.1 sh.	
		4.4	0.14
		~8	<0.1
58	$[SCN]^-$	0.0	0.29
		1.7	1.00
		3.1	2.10
		4.4	2.12
		~7	0.37
60	$[OCS]^-$	3.1	<0.1
		4.4	<0.1
64	$[S_2]^-$	0.0	<0.1
		1.2	<0.1
		3.1	<0.1
		4.6	<0.1
70	$[SCH_2CO]^-$	~5–9 broad	<0.1
71	$[SCHCO]^-$	0.0 sh.	
		1.4	0.60
		3.0	0.10
72	$[SCCO]^-$	3.2	0.18
		4.5	0.56
		~8	0.10
73	$[OCCHS]^-$	3.2	<0.1
		~4–6 broad	0.10
		~8	<0.1
74.0	m_4^*: 149 → 105	0.0 sh.	
		0.8	<0.1
74	$[OC(CH_2)S]^-$	3.2	0.10
		4.3	0.12
75	$[OC(CH_2)SH]^-$	0.0	31.8
		0.5 sh.	
76	$[CS_2]^-$	0.0 sh.	
		1.0	0.62
		3.0	<0.1
		4.3	0.10
78	$[CH_2S_2]^-$	0.0 sh.	
		1.0	0.16
		3.0	<0.1
		4.4	<0.1
86.9	m_5^*: 147 → 113	0.0	<0.1
100	$[Rdaa–COOH–CH_2S]^-$	0.0 sh.	
		1.0	<0.1
		3.1	<0.1
		~4–9 broad	<0.1
101	$[Rdaa–CO_2–CH_2S]^-$	0.0 sh.	
		1.0	0.10
103	$[CHNC(S)S]^-$	0.0 sh.	
		1.0	<0.1

Table 2 *(Continued.)*

m/e	Anion structure	Peak energy (eV)	Relative intensity
104	$[CH_2NC(S)S]^-$	0.0 sh.	
		1.1	<0.1
		3.1	<0.1
		~5–9 broad	0.17
105	$[Rdaa–H_2CCO–CO_2]^-$	0.0 sh.	
		1.2	19.2
		3.0	0.47
113	$[Rdaa–CO_2–SH_2]^-$	0.0	0.32
		0.8 sh.	
		3.1	<0.1
113.1	m_6*: 191 → 147	0.0	<0.1
114	$[Rdaa–CS_2H]^-$	0.0 sh.	
		1.5	<0.1
		3.1	<0.1
115	$[Rdaa–CS_2]^-$	0.0	0.35
		0.8	0.48
		3.1	<0.1
116	$[Rdaa–C(OH)CH_2S]^-$	0.0 sh.	
		1.2	2.35
		3.0	0.18
		4.4	0.10
117	$[Rdaa–C(O)CH_2S]^-$	1.5	0.45
118	$[Rdaa–C(O)CHS]^-$	0.0 sh.	
		1.1	0.28
		3.0	<0.1
131	$[Rdaa–CH_2COOH–H]^-$	0.0	0.10
		1.0	0.10
132	$[Rdaa–CH_2COOH]^-$	0.0	9.25
		0.8	5.59
145	$[Rdaa–CO_2–H_2]^-$	0.0	0.18
146	$[Rdaa–COOH]^-$	0.0	<0.1
		3.0	<0.1
		5.0	<0.1
147	$[Rdaa–CO_2]^-$	0.0	100
149	$[Rdaa–H_2CCO]^-$	0.0	16.6
		0.5	12.4
158	$[Rdaa–SH]^-$	0.0 sh.	
		1.1	<0.1
163	$[Rdaa–CO]^-$, 1500 μs	0.0 sh.	
		0.7	1.17
190	$[Rdaa–H]^-$	0.0 sh.	
		0.9	2.57
		1.7 sh.	
191	$[Rdaa]^-$, 200 μs	0.0	0.10

ber, together with the structures assigned in Ref. [4] to the various negative fragments.

The yield of the *m/e* = 149 anion fragment (due to loss of a neutral H_2CCO from the molecular anion) at zero energy includes a considerable isotopic contribution (9.2%) from the *m/e* = 147 anion, represented with a dotted line in Fig. 4. A weak signal with *m/e* = 191 (corresponding to the molecular anion [**Rdaa**]$^-$) was clearly observed at zero energy, as shown in Fig. 5. As found in unsubstituted **Rd**, the peak at 0.9 eV in the molecular anion current is completely accounted for by isotopic contributions (7.8%) from the relatively intense [Rdaa–H]$^-$ dehydrogenated fragment observed at *m/e* = 190.

The presence of the $–CH_2COOH$ substituent leads to a variety of complex dissociative channels upon electron attachment, including multiple fragmentations and rearrangements. In addition to those reported in Fig. 4, other anion currents detected in the 0–14 eV energy range are shown in order of decreasing yield in Figs. 5–7, where the dotted curves highlight isotopic contributions. Peak energies and relative intensities are listed in Table 2, ordered by increasing mass number. Plausible structures of the observed anion fragments are also given in Table 2.

Small fragment anions are detected also in **Rdaa**. Sulphur and hydrated sulphur fragment anions (*m/e* = 32, 33) are observed with similar shapes but inverse relative intensities with respect to the corresponding signals in **Rd**. Production of the $[CS_2]^-$ anion

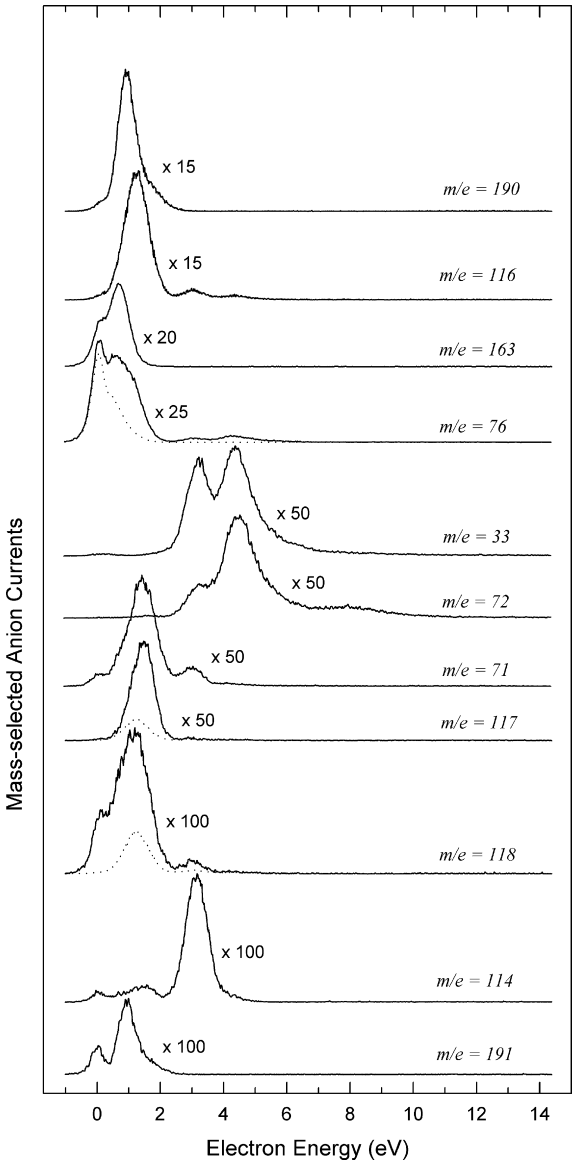

Fig. 5. Mass-selected anion currents, as a function of the incident electron energy, formed by DEA to gas-phase **Rdaa**. The intensities of these currents are smaller than that of the *m/e* = 147 current by one or two orders of magnitude. Isotopic contributions from the *m/e* = 75 to the *m/e* = 76 and from the *m/e* = 116 to the *m/e* = 117 and *m/e* = 118 yields are shown by dotted lines.

(*m/e* = 76) has a maximum at 0.9 eV, better visible once isotopic contributions (3.1%) from the *m/e* = 75 current (dotted line in Fig. 5) is subtracted. Isotopic contributions from the *m/e* = 76 peak completely account for a current observed at *m/e* = 77, but only in part for that with *m/e* = 78. The latter is likely to be ascribed to the $[CH_2S_2]^-$ fragment. The relative intensity of the $[S_2]^-$ (*m/e* = 64) current is smaller than that measured in unsubstituted **Rd**, probably because of a variety of additional (and competitive) decay channels which involve the substituent. It is not surprising that acetic acid substitution results in a strong reduction of the $[CN]^-$ (*m/e* = 26) and $[OCN]^-$ (*m/e* = 42) yields relative to those observed in **Rd**. In fact, in **Rdaa** the rearrangements that lead to their formation involve a heavy substituent group instead of a light hydrogen atom.

The *m/e* = 58 anion yield in **Rdaa** exhibits an additional distinct peak at 1.7 eV with respect to the same current measured in **Rd** (compare Figs. 2 and 4), where it was ascribed to the $[SCN]^-$ species. As a possible explanation, in **Rdaa** additional formation of $[CH_2COO]^-$ or $[CHCOOH]^-$ (plus a neutral **Rd** molecule) can occur.

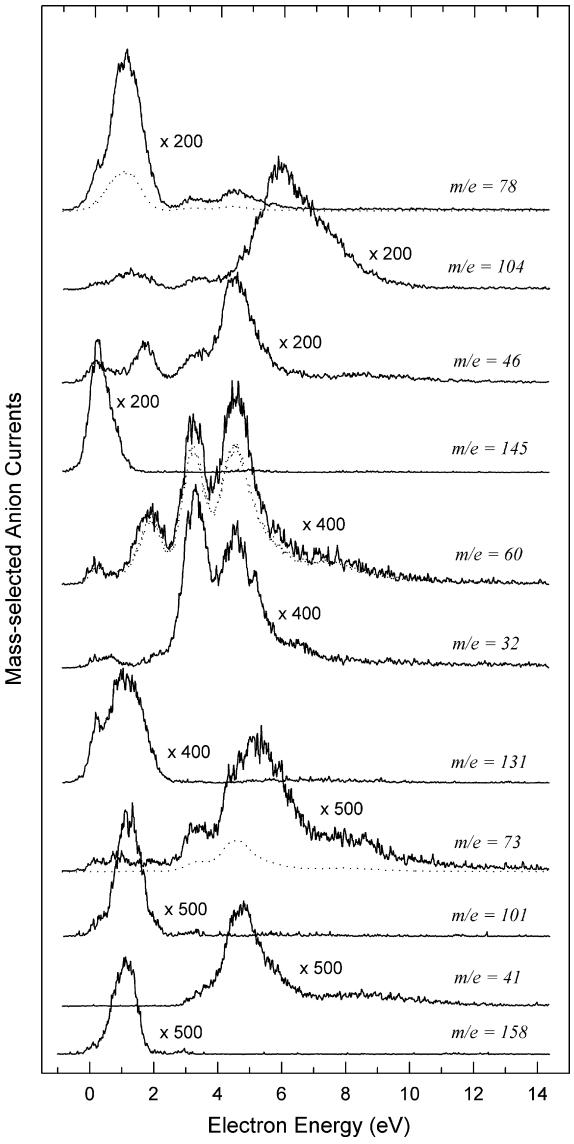

Fig. 6. Mass-selected anion currents, as a function of the incident electron energy, formed by DEA to gas-phase **Rdaa**. The intensities of these currents are smaller than that of the $m/e = 147$ current by two orders of magnitude. Isotopic contributions from the $m/e = 76$ to the $m/e = 78$, from the $m/e = 58$ to the $m/e = 60$ and from the $m/e = 72$ to the $m/e = 73$ yields are shown by dotted lines.

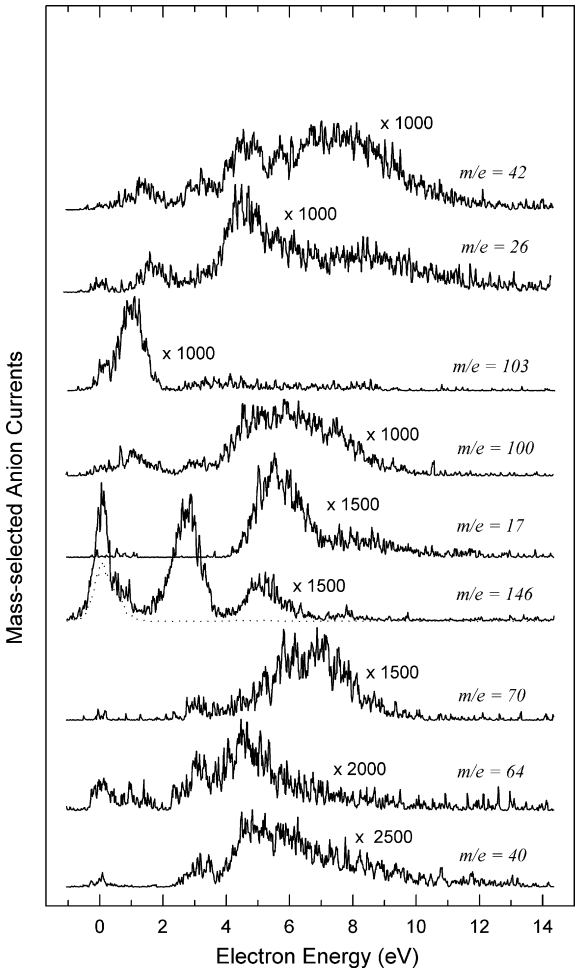

Fig. 7. Mass-selected anion currents, as a function of the incident electron energy, formed by DEA to gas-phase **Rdaa**. The intensities of these currents are smaller than that of the $m/e = 147$ current by three orders of magnitude. Isotopic contributions from the $m/e = 145$ to the $m/e = 146$ yield are shown by a dotted line.

The $m/e = 60$ anion yield seems to be somewhat higher than that expected from isotopic contribution (4.4%) from the $m/e = 58$ signal (see Fig. 6). Thus the occurrence of small yields of the $[OCS]^-$ or $[CH_2SN]^-$ fragments cannot be ruled out. As commonly observed in molecular systems which bear an OH group, a relatively weak $m/e = 17$ current peaking around 6 eV is detected also in **Rdaa** (see Fig. 7).

As found in **Rd**, also in **Rdaa** a number of complementary negative fragments (i.e., $[X]^-$ and $[M–X]^-$) are observed. The maximum yield of the $[Rdaa–SH]^-$ anion ($m/e = 158$, see Fig. 6), peaking at 1.1 eV, is shifted to 1.9 eV lower energy with respect to its counterpart ($m/e = 100$) in **Rd** (see Fig. 2). In **Rdaa** formation of this fragment can involve a hydrogen atom of the $–CH_2COOH$ group. The $m/e = 131$ current could in principle be due to formation of the $[M–OCS]^-$ fragment, i.e., the counterpart of the $m/e = 73$ signal in **Rd**. However its maxima (0.0 and 1.0 eV) are very close in energy to those of the more intense $[M–CH_2COOH]^-$ yield ($m/e = 132$), so that it seems reasonable to assign the $m/e = 131$ anion to loss of a hydrogen atom from the $m/e = 132$ anion. A relatively large yield of the $m/e = 163$ $[M–CO]^-$ negative fragment is also observed (see Fig. 5). Its shape is similar to that of its counterpart in **Rd** ($m/e = 105$), but its relative intensity is larger by an order of magnitude. In agreement, in **Rdaa** elimination of CO can take place also from the substituent. Finally, the $[M–COOH]^-$ ($m/e = 146$) and $[M–CO_2–H_2]^-$ ($m/e = 145$) currents are observed, as also found in other organic compounds containing the –COOH group (see for instance Refs. [12] and [13]).

The structures of the $m/e = 72$, 71 and 70 anion fragments are plausibly ascribed to $[SCH_2CO]^-$, $[SCHCO]^-$ and $[SCCO]^-$, respectively, because of the presence of the SCH_2CO moiety in the pentacyclic ring, although in **Rd** only the former was detected. The presence of metastable decays (discussed below) suggests that the $m/e = 75$ yield results from consecutive elimination of CO_2 from the molecular anion, to give the $m/e = 147$ negative fragment, followed by further dissociation of the latter to give $[OC(CH_2)SH]^-$ ($m/e = 75$) plus a neutral $[SCNCH_2]$ fragment. On this basis, we assign the signals with $m/e = 73$ and 74 to the $[OCCHS]^-$ and $[OC(CH_2)S]^-$ anion fragments, respectively.

A broad metastable signal around $m/e = 87$ (see below) indicates that the $m/e = 147$ anion fragment can follow a second decay channel that generates the $m/e = 113$ negative current, likely associated with the $[Rdaa–CO_2–SH_2]^-$ species. However, some contribution to the $m/e = 113$ current from the $[Rdaa–CS_2–H_2]^-$ fragment (favored on energetic grounds [4]) cannot be ruled out. One of the most intense currents ($m/e = 105$) peaks around 1 eV and corresponds to loss of a H_2CCO and a CO_2 molecule from the molecular anion,

to give the $[H_3CNC(S)S]^-$ fragment. The weak signals observed at about the same energy with $m/e = 104$ and 103 are thus ascribed to elimination of one and two hydrogen atoms, respectively, from the $m/e = 105$ fragment anion, i.e., to the structures $[CH_2NC(S)S]^-$ and $[CHNC(S)S]^-$. Plausible structures of other negative species detected in the DEA spectrum of **Rdaa** are given in Table 2.

At variance with unsubstituted **Rd**, in **Rdaa** multiple fragmentation occurs even at low energies (<2 eV), as demonstrated by several negative currents reported in Figs. 5 and 6. Some peaks are also found at higher energies, at approximately 4.4 eV ($m/e = 58$, 33 and 72) and in the 5–8 eV energy range ($m/e = 104$, see Fig. 6). These peaks are likely associated with formation of core-excited resonant anion states [3].

3.2. Slow dissociation processes

Interestingly, the negative ion mass spectra of **Rd** and **Rdaa** display several signals associated with *metastable* anions. Such species, well known in the field of mass spectrometry, give rise to unusually broad signals peaking at an apparent fractional m/e ratio. They are due to ions which dissociate in the field-free region between the accelerating region and the mass analyzer. More detailed descriptions and examples of both positive [14] and negative [15] metastable ions are available in the literature. The presence of metastable peaks in a mass spectrum indicates a slow (microsecond time scale) decomposition pathway of the initial state and supplies unambiguous information on the masses of both the initial (m_1) and final (m_2) ions according to the relation $m^* = m_2^2/m_1$, where m^* is the apparent m/e ratio of the broad metastable peak in the mass spectrum.

Fig. 8a shows portions of the negative ion mass spectrum of **Rd** recorded at fixed electron energies, indicated in the figure. The spectrum displays two metastable peaks (labeled m_1^* and m_2^* in Fig. 8a) at mass numbers $m/e = 37.0$ and 62.3. The former is assigned to decay from $m/e = 91$ to $m/e = 58$ (calculated $m^*/e = 36.97$), and the latter from $m/e = 133$ to $m/e = 91$ (calculated $m^*/e = 62.26$). The peak maxima and relative intensities of the yields of the two metastable anions are reported in Table 1.

The negative ion mass spectrum of **Rdaa** displays at least four broad peaks associated with formation of metastable anions. Fig. 8b reports the corresponding portions of the spectrum. Their mass numbers are: $m/e = 38.3$ (m_3^*), 74.0 (m_4^*), 86.9 (m_5^*) and 113.1 (m_6^*). These signals are assigned, respectively, to slow decays from $m/e = 147$ to $m/e = 75$ (calculated $m^*/e = 38.27$), from $m/e = 149$ to $m/e = 105$ (calculated $m^*/e = 73.99$), from $m/e = 147$ to $m/e = 113$ (calculated $m^*/e = 86.86$) and from $m/e = 191$ to $m/e = 147$ (calculated $m^*/e = 113.14$). The signal around $m/e = 113$ with incident electron energy close to zero, in addition to the broad contribution mentioned above, also shows a sharp contribution (see Fig. 8b) not associated with metastable anions. The mass peak at $m/e = 74$ recorded with 4.3 eV incident electron energy is normally shaped, whereas the broad $m/e = 74$ peak recorded with 0.8 eV electron energy is clearly due to a metastable anion. The detection of the metastable channel m_3^*, associated with slow $m/e = 147 \rightarrow m/e = 75$ dissociation, is perfectly consistent with the previous observation [4] of a strong temperature dependence of the relative intensities of these fragment anions.

3.3. Electron detachment times

A final aspect of the present experimental results deals with the survival time of temporary anions with respect to detachment of the extra electron. The molecular anions of both **Rd** and **Rdaa** were observed with microsecond lifetimes at an incident electron energy close to zero. These findings are not surprising because both molecules possess a fairly large adiabatic electron affinity (about 0.7 eV [4]) and many vibrational states over which the excess energy can be distributed. According to the present measurements, the electron detachment times from the molecular anions of **Rd** and **Rdaa** are 30 μs and 250 μs at zero energy, respectively, to be compared with a reference detachment time from $[SF_6]^-$ of 120 μs under the same experimental conditions. In both cases the isotopic contributions from the dehydrogenated fragment anion to the yield of the molecular anion are too small to affect the measurements. The detachment time from the molecular anion of **Rdaa** is larger than that from **Rd** by an order of magnitude, in line with a larger number of vibrational degrees of freedom and a slightly higher adiabatic electron affinity in the former.

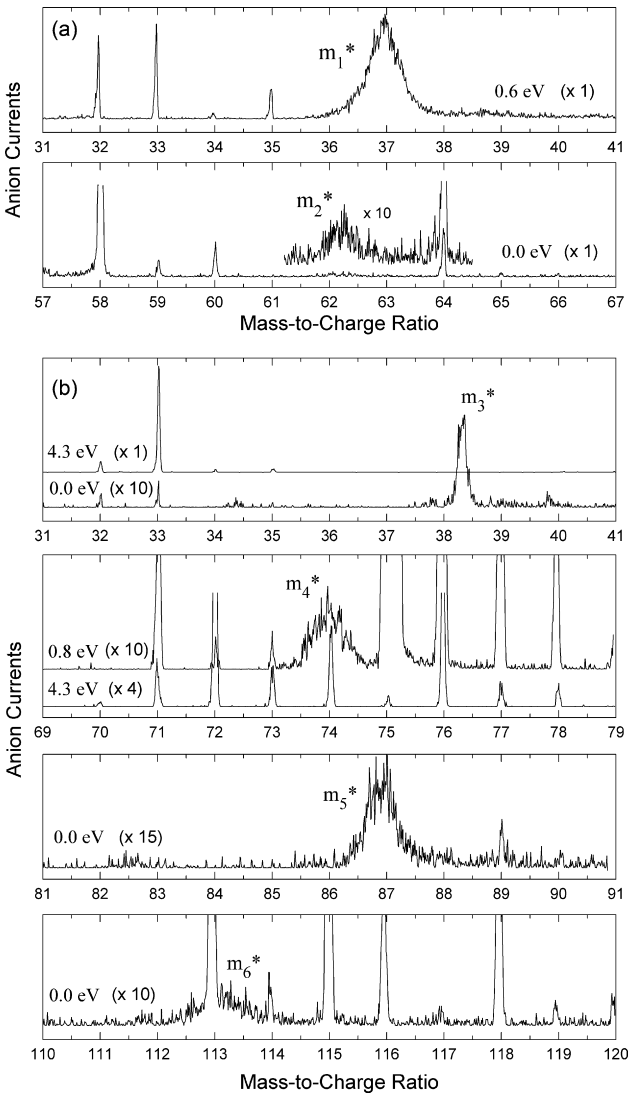

Fig. 8. Sections of the negative ion mass spectrum recorded at fixed incident electron energies (indicated in the figure), showing the metastable decays m_1^*, m_2^* in **Rd** (a) and m_3^*, m_4^*, m_5^*, m_6^* in **Rdaa** (b).

The fragment negative ion observed at $m/e = 163$ in **Rdaa**, with a shoulder at zero energy and a maximum at 0.7 eV, was found to detach the extra electron in about 1500 μs at 0.7 eV, whereas electron detachment in the time window of our apparatus was not observed at zero energy. The lifetimes of closed-shell fragment anions (formed by electron addition to a neutral radical fragment) are usually much higher. In agreement, the $m/e = 163$ anion yield is ascribed to formation of the $[M–CO]^-$ species, i.e., the molecular anion of rhodanine N-substituted by a CH_2OH group (rhodanine-

Chart 2.

Table 3
B3LYP/6–31+G(d) total electronic energies (eV) relative to the ground neutral state of rhodanine-3-acetic acid and (between parentheses) with zero-point vibrational energy corrections.

	Total energy
Rdhm + CO	1.089 (0.965)
$[Rdhm]^-$ + CO	0.250 (0.058)

3-hydroxymethyl, **Rdhm**, see Chart 2).

Table 3 reports the thermodynamic energy thresholds calculated at the B3LYP/6–31+G(d) level of theory for the loss of a CO neutral molecule from **Rdaa**, to give **Rdhm** or $[Rdhm]^-$. Once the total electronic energies are corrected accounting for the zero-point vibrational energies, the threshold for production of the $[Rdhm]^-$ anion results to be very close to zero, in agreement with the $m/e = 163$ signal observed at zero energy. However, the maximum of this current occurs at 0.7 eV. This findings suggest that the loss of a CO molecule from the $[Rdaa]^-$ molecular anion is not associated with its electronic ground state, but with the anion formed (around 1 eV [4]) by electron capture into the empty π^* MO mainly localized on the carbonyl group of the CH_2COOH substituent. The calculated data of Table 3 also lead to an adiabatic electron affinity of 0.907 eV (including zero-point corrections) for the **Rdhm** molecule.

4. Discussion

The present gas-phase DEA investigation shows that low-energy electron attachment to **Rd** and **Rdaa** is followed by a great variety of dissociative channels. Interestingly, numerous *metastable* decays of temporary negative ions are also observed. In particular, these slow dissociation processes are involved in the formation of all the most intense negative fragments. Scheme 1 reports fragmentation channels of the initially formed temporary molecular anion of **Rd**, where the widths of the arrows give a qualitative representation of the relative intensities of the corresponding decay channels. The

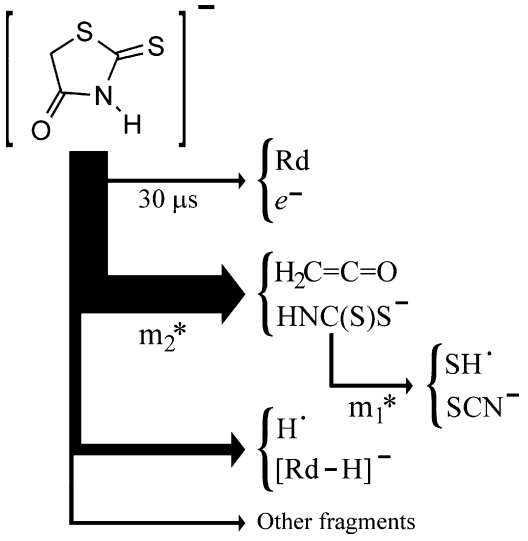

Scheme 1.

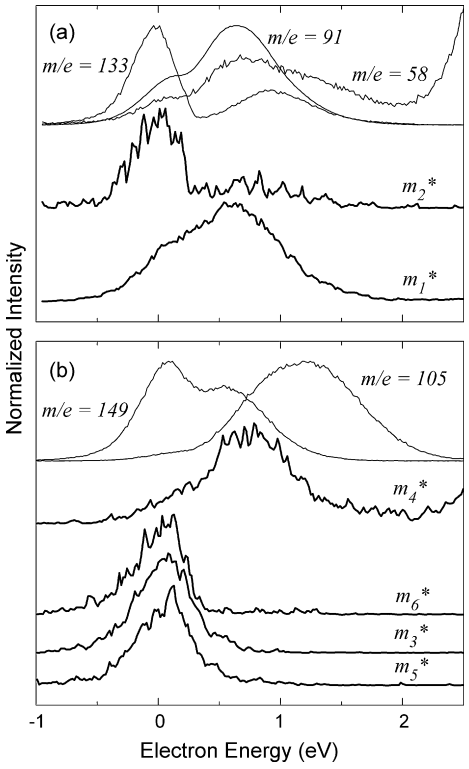

Fig. 9. Mass-selected anion currents, as a function of the incident electron energy, corresponding to the metastable decays observed in **Rd** (a) and **Rdaa** (b). All currents are normalized to equal intensity.

most intense pathway of $[Rd]^-$ decomposition consists of two slow consecutive decays (labeled m_2^* and m_1^* in Scheme 1), the latter having a smaller relative intensity (by two orders of magnitude).

Strictly speaking, the observable contributions (i.e., intensities of the $m/e = 62.3$ and 37.0 signals relative to those of the $m/e = 91$ and 58 counterparts, respectively) of metastable anions to these dissociation pathways are small. However, under the present experimental conditions, the time of anion extraction from the collision cell is estimated to be approximately 12 μs, so that even the "normal" anion fragments (observed as narrow mass peaks) may be formed "slowly" inside the collision cell. In fact, formation of the $[Rd–H_2CCO]^-$ anion fragment ($m/e = 91$) requires rupture of two bonds of the **Rd** ring, followed by formation of a new bond in the ketene neutral fragment. Such a complex rearrangement can hardly take place as quickly as a simple single-bond dissociation. Similarly, the following loss of an SH neutral radical from the $m/e = 91$ fragment also requires strong (and slow) rearrangements. It seems thus reasonable that all the $m/e = 91$ and 58 fragment anions must be formed slowly at the same energies (around zero and 0.6 eV) where the corresponding metastable yields (m_1^* and m_2^*, see Table 1 and Fig. 9) are experimentally observed.

Owing to the acetic acid substituent, the fragmentation picture of the temporary molecular anion of **Rdaa** is notably more complex, as shown in Scheme 2. As observed in **Rd**, elimination of a neutral ketene molecule occurs also in **Rdaa**, although with a smaller relative intensity. Even in the case of **Rdaa** this dissociation (which requires cleavage of at least two bonds) is expected to be slow, although a corresponding metastable peak (calculated $m^*/e = 116.24$, labeled m_7^* in Scheme 2) was not experimentally detected. The next step of this dissociative channel is the observed metastable loss of a CO_2 molecule (labeled m_4^*). These findings indicate that the $[Rdaa–H_2CCO]^-$ anion formed from **Rdaa** is less stable then its counterpart in **Rd**. In fact, only a small fraction of the latter undergoes further dissociation (see Scheme 1), while the

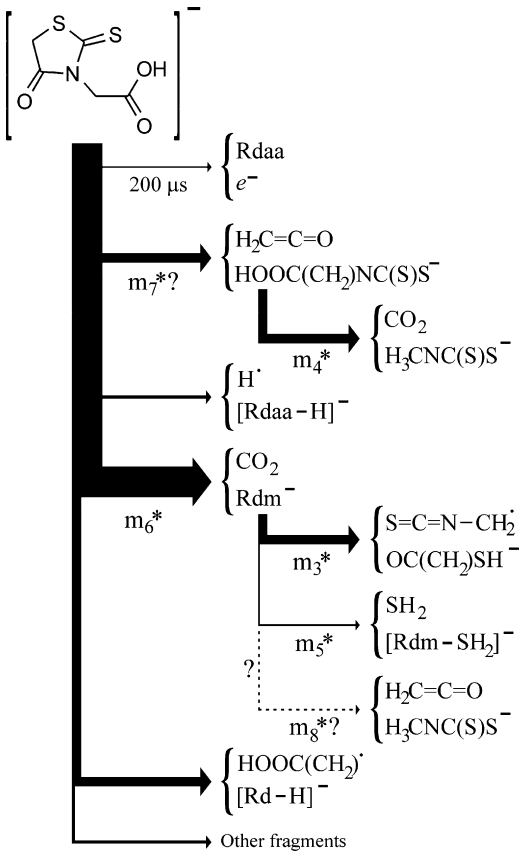

Scheme 2.

former dissociates almost completely to give $[H_3CNC(S)S]^-$ and a CO_2 molecule, as indicated in Scheme 2.

At variance with $[Rd]^-$, the most probable dissociation pathway of $[Rdaa]^-$ consists in the elimination of a CO_2 molecule to give the rhodanine-3-methyl (**Rdm**, see Chart 2) negative ion. A plausible additional dissociation step of $[Rdm]^-$, marked with a dashed line in Scheme 2, consists in the elimination of a neutral ketene molecule, i.e., a pathway alternative to the dissociation branch labeled m_4^* in Scheme 2, leading to the same final products (ketene, CO_2 and $[H_3CNC(S)S]^-$). A corresponding metastable peak at an apparent mass of 75.00 (labeled m_8^* in Scheme 2) could not be detected. However, its presence would likely be masked by the intense $m/e = 75$ signal observed at zero incident electron energy. Besides, elimination of a ketene molecule from the **Rdm** molecular anion could be too slow to be detected as a metastable dissociation under the present experimental conditions. Other observable pathways of slow decomposition of $[Rdm]^-$ are labeled m_3^* and m_5^* in Scheme 2, the latter being an order of magnitude less intense. Following the same considerations made above for **Rd**, all the fragments of **Rdaa** involved in the branches labeled as m_3^*, m_4^*, m_5^* and m_6^* in Scheme 2 imply the occurrence of complex rearrangements and their formation is thus believed to occur slowly.

Some more insight into consecutive dissociation pathways of **Rd** and **Rdaa** temporary molecular anions may be obtained from comparison of the yield shapes, as a function of the incident electron energy, for anions involved in metastable processes. Fig. 9 shows anion yields (normalized to equal intensities) in **Rd** (panel a) and **Rdaa** (panel b). The m_1^* (in **Rd**) and m_4^* (in **Rdaa**) yields peak at 0.6 and 0.8 eV, respectively (see Tables 1 and 2). These values are close to the energies (0.84 and 1.14 eV in **Rd**, 0.97 and 1.07 eV in **Rdaa**) of vertical electron attachment to the second and third empty MOs, with mainly σ^*_{CS} and ring π^*_{CO} character, respectively [4]. The shift to lower energy of the DEA peaks relative to the corresponding shape resonances (observed in ETS) is well understood in terms of the survival probability factor of temporary anions [16]. Therefore, electron attachment to the LUMO+1 and/or LUMO+2 (in **Rdaa** also LUMO+3, with mainly π^*_{COOH} character [4], could be involved) is likely the first step of a mechanism which leads to slow metastable dissociation, occurring in the microsecond time scale. The lifetime (with respect to detachment of the added electron) of shape resonances at this energy is smaller by many orders of magnitude. This indicates that the initially formed excited anion state can rapidly convert to its electronic ground state, distributing the excess energy into vibrational modes. This anion species would then survive long enough to lose consecutively a neutral ketene molecule and an SH radical in the case of **Rd**, or a ketene and a carbon dioxide molecule in **Rdaa**. Since the metastable decay m_1^* follows m_2^* (see Scheme 1), also m_2^* should be associated with electron capture into the LUMO+1 and/or LUMO+2 of **Rd**. Consistently, a small signal in the m_2^* yield is observed around 0.6 eV (see Fig. 9).

The m_1^*, m_2^* (in **Rd**) and m_4^* (in **Rdaa**) decay channels are detected also at zero energy, following electron attachment to the mainly π^*_{CS} [4] LUMO to give the (vibrationally excited) first anion state. The signals from the metastable processes labeled m_3^*, $m_5^*$and m_6^* peak only at zero energy (see Fig. 9). The dissociation branches m_2^* and m_6^* are associated with formation of the most intense fragment anions observed in the DEA spectra of **Rd** ($m/e = 91$) and **Rdaa** ($m/e = 147$), respectively. It can be noted that formation of a specific negative fragment can occur even when the total energy (only electronic contributions) of the products of dissociation is somewhat higher than that of the target neutral molecule plus the incident electron. Slow dissociation, in fact, allows for energy redistribution over the vibrational degrees of freedom, so that part of the excess vibrational energy can be spent for dissociation, generating (charged and neutral) "cooled" fragments.

The thermodynamic threshold (only electronic contributions) supplied by B3LYP/6–31+G(d) calculations for formation of the $m/e = 91$ anion plus a neutral $H_2C{=}C{=}O$ molecule is 0.434 eV [4]. We used the same theoretical method to include the vibrational zero-point energy. This correction reduces the evaluated thermodynamic threshold to only 0.180 eV. Formation of the $m/e = 91$ fragment, in fact, is observed also at zero energy (see Fig. 1, in agreement with previous work [4]). Assuming the reliability of the calculated energy threshold, the appearance of the $[HNC(S)S]^-$ fragment ($m/e = 91$) at zero incident electron energy is possible if a portion of the vibrational energy (not accounted for by the calculations) of rhodanine at 80 °C can be concentrated on a suitable degree of freedom. Such an energy redistribution requires a relatively long time and a correspondingly slow dissociation. According to the calculations the $[Rdm]^-$ anion plus a neutral CO_2 molecule are largely (>1 eV) more stable than a neutral **Rdaa** molecule [4], so that formation of the $m/e = 147$ anion fragment does not rely on the excess of vibrational energy of the target molecule.

5. Conclusions

Dissociative electron attachment to gas-phase rhodanine (**Rd**) and rhodanine-3-acetic acid (**Rdaa**) has been investigated in the 0–14 eV energy range. In both compounds, only a small yield of molecular anion is observed at zero incident electron energy. The lifetime of these molecular anions with respect to detachment of the added electron has been experimentally determined to be about 30 μs and 200 μs for **Rd** and **Rdaa**, respectively. This long survival time is in line with the possibility to undergo complex (and thus relatively slow) dissociation processes. Consistently, slow dissoci-

ation of metastable anions (occurring in the first field-free region on a microsecond time scale) are detected at zero energy.

A variety of negative fragment currents are observed at incident electron energies <1 eV, most of which imply the occurrence of multiple bond ruptures and structural rearrangements. Such processes require that the dissociating temporary anions possess a long survival time with respect to detachment of the extra electron. In agreement, formation of metastable anions is also observed above zero energy. It is concluded that the (electronically excited) molecular anions formed by electron capture into the LUMO+1 or LUMO+2 (their typical lifetime with respect to autodetachment of the extra electron is 10^{-13} to 10^{-14} s) can quickly relax into the (vibrationally excited) ground anion state, where the whole excess energy can be redistributed over many available vibrational modes. This species would then survive long enough to undergo dissociation process on the microsecond time scale.

The species detected as products of slow metastable dissociations also include the most intense fragment anions found in the DEA spectrum of **Rd** (loss of a ketene molecule from the molecular anion) and **Rdaa** (loss of a CO_2 molecule from the molecular anion). The presence of the substituent in **Rdaa** opens a variety of additional dissociative channels with respect to unsubstituted **Rd**. With the support of the observed metastable anions, detailed fragmentation schemes (which also include consecutive processes) are proposed to account for the main dissociation mechanisms of the molecular anions.

Rdaa has been successfully used as an electron-acceptor anchored to TiO_2 in dye-sensitized solar cells [1]. According to the present gas-phase DEAS results, the requirement of long-term stability can be hardly fulfilled under conditions of excess negative charge. However, it is to be noted that in the condensed phase stabilizing interactions with neighboring molecules can strongly influence the decay mechanisms of the molecular anion, and possibly reduce its dissociative cross-section [17]. For instance, it was recently found [18] that electron attachment to trinitrotoluene embedded into helium droplets does not generate the various fragmentation product observed in the gas phase. Moreover, the present investigation shows that the most intense dissociation channels of the **Rdaa** molecular anion are slow, so that a rapid injection of negative charge from the excited dye into the conduction band of TiO_2 might also contribute to prevent decomposition.

Acknowledgement

A.M. thanks the Italian Ministero dell'Istruzione, dell'Università e della Ricerca for financial support.

References

[1] M. Liang, W. Xu, F. Cai, P. Chen, B. Peng, J. Chen, Z. Li, J. Phys. Chem. C 111 (2007) 4465.
[2] L. Sanche, G.J. Schulz, Phys. Rev. A 5 (1972) 1672.
[3] G.J. Schulz, Rev. Mod. Phys. 45 (1973) 378, 423.
[4] A. Modelli, D. Jones, S.A. Pshenichnyuk, J. Phys. Chem. C 114 (2010) 1725.
[5] V.I. Khvostenko, Negative Ions Mass Spectrometry in Organic Chemistry, Moscow, Nauka, 1981 (in Russian).
[6] S.A. Pshenichnyuk, N.L. Asfandiarov, Eur. J. Mass Spectrom. 10 (2004) 477.
[7] D. Edelson, J.E. Griffiths, K.B. McAfee Jr., J. Chem. Phys. 37 (1962) 917.
[8] [8] M.J. Frisch, G.W. Trucks, H.B. Schlegel, G.E. Scuseria, M.A. Robb, J.R. Cheeseman, J.A. Montgomery, T. Vreven, K.N. Kudin, J.C. Burant, J.M. Millam, S.S. Iyengar, J. Tomasi, V. Barone, B. Mennucci, M. Cossi, G. Scalmani, N. Rega, G.A. Petersson, H. Nakatsuji, M. Hada, M. Ehara, K. Toyota, R. Fukuda, J. Hasegawa, M. Ishida, T. Nakajima, Y. Honda, O. Kitao, H. Nakai, M. Klene, X. Li, J.E. Knox, H.P. Hratchian, J.B. Cross, V. Bakken, C. Adamo, J. Jaramillo, R. Gomperts, R.E. Stratmann, O. Yazyev, A.J. Austin, R. Cammi, C. Pomelli, J.W. Ochterski, P.Y. Ayala, K. Morokuma, G.A. Voth, P. Salvador, J.J. Dannenberg, V.G. Zakrzewski, S. Dapprich, A.D. Daniels, M.C. Strain, O. Farkas, D.K. Malick, A.D. Rabuck, K. Raghavachari, J.B. Foresman, J.V. Ortiz, Q. Cui, A.G. Baboul, S. Clifford, J. Cioslowski, B.B. Stefanov, G. Liu, A. Liashenko, P. Piskorz, I. Komaroni, R.L. Martin, D.J. Fox, T. Keith, M.A. Al-Laham, C.Y. Peng, A. Nanayakkara, M. Challacombe, P.M.W. Gill, B. Johnson, W. Chen, M.W. Wong, C. Gonzalez, J.A. Pople, Gaussian 03, Revision D.01, Gaussian Inc., Wallingford, CT, 2004.
[9] A.D. Becke, J. Chem. Phys. 98 (1993) 5648.
[10] S.A. Pshenichnyuk, G.A. Gallup, B.D. Burrow, J. Phys. Chem. A 111 (2007) 11837.
[11] R.E. Stratmann, G.E. Scuseria, M.J. Frisch, J. Chem. Phys. 109 (1998) 8218.
[12] S.A. Pshenichnyuk, N.L. Asfandiarov, V.S. Fal'ko, V.G. Lukin, Int. J. Mass Spectrom. 227 (2003) 259.
[13] A. Pelc, W. Sailer, P. Scheier, N.J. Mason, E. Illenberger, T.D. Mark, Vacuum 70 (2003) 429.
[14] J.A. Hipple, R.E. Fox, E.U. Condon, Phys. Rev. 69 (1946) 347.
[15] B.L. Donnally, H.E. Carr, Phys. Rev. 93 (1954) 111.
[16] T.F. O'Malley, Phys. Rev. 150 (1966) 14.
[17] R. Balog, J. Langer, S. Gohlke, M. Stano, H. Abdoul-Carime, E. Illenberger, Int. J. Mass Spectrom. 233 (2004) 267.
[18] A. Mauracher, H. Schöbel, F.F. da Silva, A. Edtbauer, C. Mitterdorfer, S. Denifl, T.D. Märk, E. Illenberger, P. Scheier, Phys. Chem. Chem. Phys. 11 (2009) 8240.